

Sonic Hedgehog Is Required for the Assembly and Remodeling of Branchial Arch Blood Vessels

Hana Kolesová,¹ Henk Roelink,^{2*} and Miloš Grim¹

Sonic hedgehog (Shh) is a morphogen involved in many developmental processes. Injection of cells (5E1) that produce a Shh-blocking antibody causes an attenuation of the Shh response, and this causes vascular malformations and impaired remodeling characterized by hemorrhages and protrusions of the anterior cardinal vein and outflow tract, delayed fusion of the dorsal aortae, impaired branching of the internal carotid artery, and delayed remodeling of the aortic arches. Distribution of smooth muscle cells in the vessel wall is unchanged. In 5E1-injected embryos, we also observed impaired assembly of endothelial cells into vascular tubes, particularly in the sixth branchial arch, around the anterior cardinal vein and around the dorsal aorta. In 5E1-treated embryos, increased numbers of macrophage-like cells, apoptotic cells, and a decreased level of proliferation were observed in head mesenchyme. Together, these observations show that Shh signaling is required at multiple stages for proper vessel formation and remodeling. *Developmental Dynamics* 237:1923–1934, 2008. © 2008 Wiley-Liss, Inc.

Key words: Shh; blood vessels; branchial arches; 5E1 hybridoma cells; quail embryo; endothelium

Accepted 8 May 2008

INTRODUCTION

The inductive events controlling the formation and remodeling of the first intra-embryonic vessels are not well understood. Classical embryological experiments have demonstrated that signals derived from endoderm can induce vessel formation in adjacent mesoderm (Pardanaud et al., 1989), and it appears that the Hedgehog (Hh) signaling mediates at least some of this endoderm-derived activity since *Smo* null embryos, which cannot respond to Hedgehog (Hh), exhibit severe vascular defects (Byrd et al., 2002). Embryos treated at later stages with the

Smo inhibitor cyclopamine show defects in vascular remodeling (Nagase et al., 2006), indicating an ongoing requirement for Hh signaling.

Among the first intraembryonic vessels induced by endodermally derived signals are the vessels of the branchial (pharyngeal) region. Mouse embryos lacking *Shh* have hypoplastic first branchial arches that prematurely fuse in the midline (Yamagishi et al., 2006). The second and third branchial arches are hypoplastic, while the fourth and sixth arches do not appear to develop at all (Washington Smoak et al., 2005). *Smo* null embryos die too

early to assess the role for Hedgehog signaling for pharyngeal vessel development (Zhang et al., 2001; Wijgerde et al., 2002).

Vessels of the branchial region undergo extensive remodeling in stages 15 to 23. At stage 15, caudal parts of the paired aortae fuse to form a single descending aorta, while rostrally they become the distal parts of the left and right internal carotid arteries. The ventral aorta after the branching into the aortic arches continues as the left and right external carotid arteries.

The first to sixth aortic arches develop in a cranio-caudal gradient (Hi-

¹Institute of Anatomy, First Faculty of Medicine, Charles University, Prague, Prague, Czech Republic

²Department of Molecular and Cell Biology, University of California at Berkeley, Berkeley, California
Grant sponsor: Charles University; Grant number: GAUK 54/203209; Grant sponsor: NIH; Grant number: 1R01HD042307; Grant sponsor: The Ministry of Education of The Czech Republic; Grant number: MSM 0021620806.

*Correspondence to: Henk Roelink, Department of Molecular and Cell Biology, University of California at Berkeley, Berkeley, CA 94720-3204. E-mail: roelink@berkeley.edu

DOI 10.1002/dvdy.21608

Published online 21 June 2008 in Wiley InterScience (www.interscience.wiley.com).

ruma and Hirakow, 1995) from stages 12 to 23. They form in branchial arch mesenchyme from cords of angioblasts around the foregut, which subsequently become luminized and serve as a communication between the ventral and dorsal aorta. In fish and amphibian larvae, most branchial arches develop into the gill arches (Kolesova et al., 2007); in amniotes, aortic arches undergo significant remodeling.

The first, second, and fifth aortic arches undergo regression that starts at stage 21. The third, fourth, and sixth aortic arches are gradually rearranged. The third aortic arch is incorporated into the common and internal carotid arteries. In birds, the right fourth arch contributes to the arch of aorta. The remainder of the left one incorporates in the subclavian artery. The sixth aortic arch becomes part of the pulmonary artery. The main veins of the cranial region are the paired anterior cardinal veins, which drain blood from the head and neck to the common cardinal vein. The anterior cardinal veins develop at stage 12.

The endothelial cells lining the vessels in the branchial region originate from paraxial mesoderm (Noden and Trainor, 2005; Evans and Noden, 2006). Initially, presumptive vessels consist of an endothelial lining, which

is subsequently covered with a layer of smooth muscle cells. The dorsal aorta is covered by sclerotome-derived cells (Wiegrefe et al., 2007), the aortic arches by cells derived from the neural crest (Le Lievre and Le Douarin, 1975). Shh can induce angiogenic factors such as VEGFs and Angiopoietins in mesenchyme (Pola et al., 2001) and thus affect the smooth muscle distribution and vessel stabilization (van Tuyl et al., 2007). The anterior cardinal veins have no smooth muscle layer.

The aortic arches are located within the corresponding branchial arches, which are formed from neural crest cells and cells of paraxial mesoderm and are lined with an ectoderm on the outside, and endoderm on the surfaces surrounding the developing pharynx. Endothelial cells and striated muscle cells are derived from mesoderm, while other tissues in the branchial arches are of neural crest origin (Evans and Noden, 2006). According to some observations, mesenchymal cells of branchial arches are stimulated to proliferate and prevented from apoptosis by Shh (Ahlgren and Bronner-Fraser, 1999; Jeong et al., 2004).

We tested the requirement for Shh for the correct development of the ves-

sels associated with the branchial arches, and found that decreased levels of Shh signaling result in angiogenic malformations. Ongoing development of existing vessels is disrupted by attenuated Shh signaling. These vessels lose their ability to remodel, fuse, and form branches. The vessel walls, in particular of the anterior cardinal veins, appear to be malformed; hemorrhages are common in this area, and these vessels cannot contain ink. The area around the anterior cardinal veins has increased levels of apoptotic cells and macrophage-like cells. Moreover, new vessel formation is impaired, and endoderm cells can often be seen lining incomplete vessels, or as aggregates. Altogether, our results demonstrate a varied and continual requirement for Shh signaling in the development of the vessels in and around the branchial arches.

RESULTS

Vessel Formation in Branchial Arches

The development of vessels in the branchial region was extensively described in chicken embryos (Hiruma and Hirakow, 1995), and is very similar in the quail embryo, although the

Fig. 1. A–D: Normal development of head and neck vessels in quail embryos. Vessels stained with QH1 Ab. E–F: Expression of Shh, visualized with 5E1 Ab. **A:** A stage-15 embryo with a formed first aortic arch (I), which connects the ventral (VA) with the dorsal aorta (DA). The anterior cardinal vein is also indicated (CV). **B:** Stage 18, with the second (II), third (III), and the fourth (not visible on this section) aortic arches indicated. The anterior part of the dorsal aorta (DA) continues as the internal carotid artery (IC). **C:** At stage 21, the fourth (IV) aortic arch is indicated. **D:** Stage 23, with the fifth (V) and sixth (VI) aortic arches. **E,F:** Shh expression visualized with anti-Shh antibody in normal embryos. Stage 15 (E), stage 18 (F). Shh expression is visible in the notochord, floor plate (arrows), and foregut (E, arrowheads) and parts of the branchial arch endoderm (F, arrowheads). Transversal sections. D–F are counterstained with hematoxylin. Scale bar = 400 μ m in all panels.

Fig. 2. Inhibition of the Shh response by 5E1 (anti-Shh) Ab produced by hybridoma cells. A,B: Sections of stage-18 embryos injected at stage 11 with hybridoma cells. Sections incubated with secondary antibody. **A:** An embryo injected with control 12CA5 hybridoma cells. No staining is visible in the embryo. Secondary antibody reacts with hybridoma cells (arrowheads). **B:** An embryo injected with 5E1 hybridoma cells producing anti-Shh antibody. Shh-expressing structures, floor plate, notochord, and endoderm of the branchial arches are indicated (arrows). Hybridoma cells are also stained (arrowheads). Counterstained with hematoxylin. Scale bar = 400 μ m in both panels. C,D: Expression of *Ptch1*, which is induced in response to Shh signaling. **C:** An embryo injected with 12CA5 hybridoma cells shows normal distribution of *Ptch1* in the ventral part of the neuroepithelium, in the endoderm of branchial arches, and in adjacent mesenchyme (arrows). **D:** An embryo injected with 5E1 hybridoma cells shows a decreased level of *Ptch1* expression. Residual expression is observed only in the ventral part of the nervous system and in a few areas of branchial arch endoderm (arrows). No expression is detected in the mesenchyme. Scale bar = 200 μ m in both panels.

Fig. 3. Ink injection into blood vessels at stage 18. **A:** In a 12CA5-injected control embryo, the first and the second aortic arches have regressed and formed capillary plexuses (white arrows I, II). The main artery conducting blood from the heart to the dorsal aorta is the third aortic arch in this stage (white arrow III). The fourth aortic arch starts to develop (white arrow IV). Normal capillary plexuses drained into anterior cardinal vein are visible in the head. **B:** Embryo injected with 5E1 hybridoma cells has a smaller head compared to the control. Development of the aortic arches is delayed. The first and the second aortic arches are still present and form functional communication between the heart and the dorsal aorta (white arrows I, II). The third and the fourth aortic arches are normally developed (white arrows III, IV). A significant amount of ink has leaked from the tributaries to the anterior cardinal vein (white arrowheads). Scale bar in A and B = 500 μ m. C, D: Paraffin sections of the anterior cardinal vein region, stained for acid phosphatase. N, neuroepithelium. **C:** Red blood cells (arrowheads) are visible only in vessels; macrophage-like cells are indicated (arrow). **D:** Red blood cells localized extravascularly (arrowheads), macrophage-like cells are more numerous than in control embryos (arrow). Scale bar in C and D = 200 μ m.

timing of their development is somewhat different. Generally, in quail embryos the aortic arches remodel faster; they form approximately one stage later, and they regress a few stages earlier than in chick embryos. At

stage 15, the first aortic arch is present as a vessel connecting the ventral and dorsal aorta, and the anterior cardinal vein is already developed (Fig. 1A). Immediately after the first aortic arch has formed, the sec-

ond arch starts to develop. The third aortic arch develops around stage 18 (Fig. 1B) and the fourth one develops at stage 20. At stage 21, the fifth and sixth aortic arches start to develop and are fully formed at stage 23 (Fig. 1C,D). The first and second aortic arches start to regress at stage 18. The fifth aortic arch, a minor bypass of the sixth aortic arch, starts to regress at stage 24. While the first, second, and fifth aortic arches are transient structures, the third, fourth, and sixth arches persist.

At stage 15, only the aortic arches

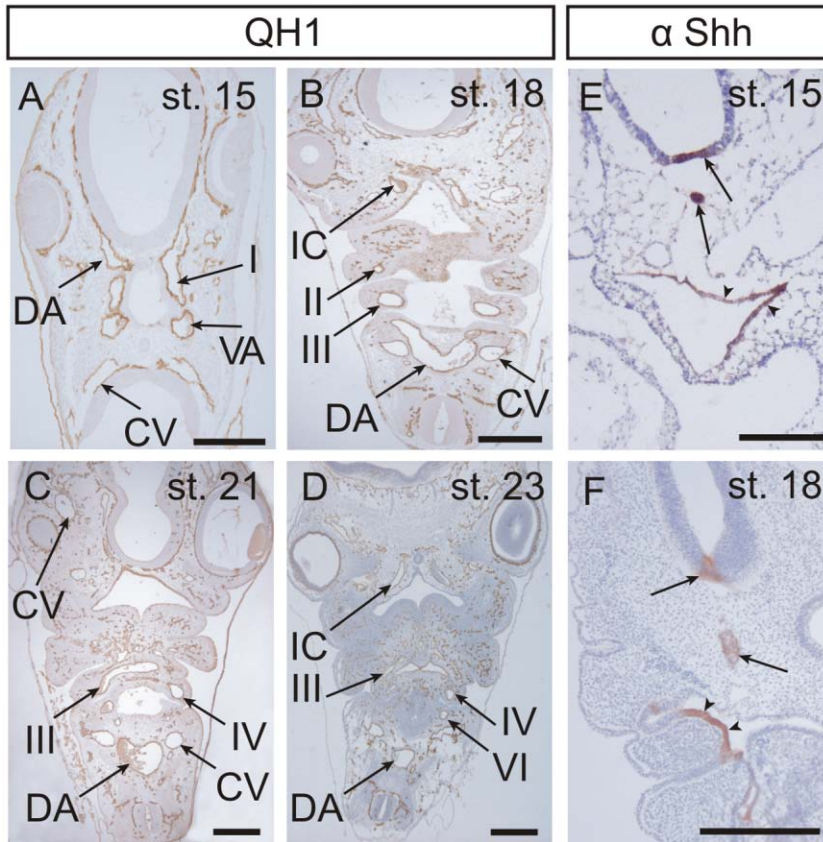


Fig. 1.

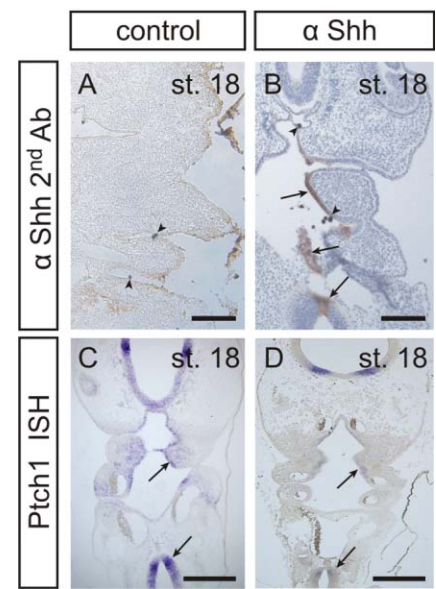


Fig. 2.

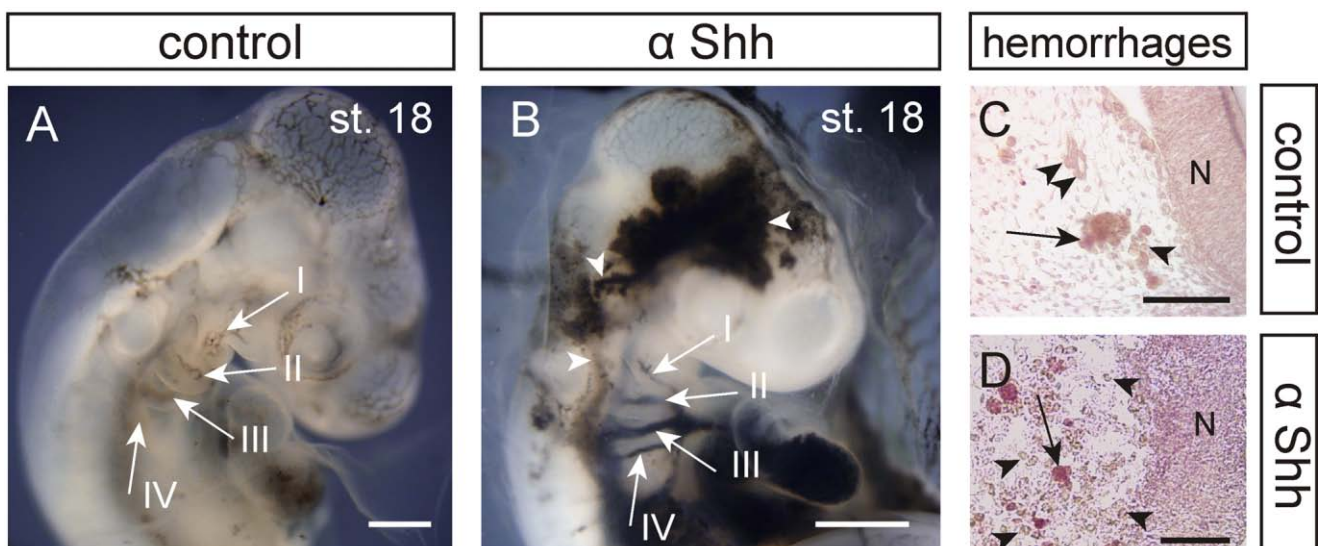


Fig. 3.

supply the branchial arches (Fig. 1A), while at stage 18, the dorsal aorta, the aortic arches, as well as the anterior cardinal vein give off smaller branches and capillaries (Fig. 1B). At stages 21 and 23, the development of small vessels and capillaries continues in the whole region, resulting in a dense capillary network in branchial arch mesenchyme and in the regions surrounding the brain and eyes (Fig. 1C,D).

Besides luminized vessels and capillaries, we also observed an increasing number of isolated angiogenic cells at stages 18–23 (Fig. 1B–D). These cells are mainly present around the anterior cardinal vein and in branchial arches, while in the area in the vicinity of the dorsal aorta, only a few of these cells are detected. These isolated angiogenic cells are evenly distributed in the mesenchyme.

Inhibition of Shh Signaling With Anti-Shh Antibodies Produced by 5E1 Hybridoma Cells

In general, we detected Shh in a pattern and timing consistent with that observed in the chick (Roelink et al., 1995). The notochord is a prominent site of early expression, and starting at stage 15, Shh is expressed in endoderm lining the branchial arches and the foregut (Fig. 1E,F). To conditionally attenuate Shh signaling, we injected 5E1 (anti-Shh) hybridoma cells under the vitelline membrane of stage-10–12 embryos, which were analyzed at stages 18–23. 5E1 hybridoma cell-derived anti-Shh antibodies distribute widely in injected embryos. Visualizing the 5E1 antibodies by simply using an anti-IgG secondary antibody on sectioned embryos, staining is detected at the sites of *Shh* expression, such as the notochord, floor plate, and endoderm of the branchial arches and foregut. The secondary antibodies also react with 5E1 hybridoma cells, which always remain at the embryonic surface (Fig. 2A,B), just as the control 12CA5 hybridoma cells (Fig. 2C,D).

To verify if the Shh response is efficiently blocked after 5E1 injection, we analyzed the expression of the gene coding for its receptor *Ptch1* by mRNA in situ hybridization. *Ptch1* expres-

sion is invariably upregulated in response to Shh signaling (Marigo and Tabin, 1996). In control embryos, *Ptch1* is expressed in areas adjacent to Shh sources, such as branchial arch mesenchyme, around the foregut, in the ventral part of the neural tube, and around domains of Shh production in the brain (Fig. 2C). In embryos injected with 5E1 cells, *Ptch1* expression in the neural tube and endoderm is decreased and no *Ptch1* expression is found in the abutting mesenchyme (Fig. 2D), demonstrating a significant attenuation of the Shh response. Residual expression of *Ptch1* could be the result of incomplete inhibition, but also be caused by other Hh ligands, which are not recognized by 5E1 (Goodrich et al., 1997; Carpenter et al., 1998).

Embryos injected with 5E1 and with control 12CA5 hybridoma cells develop slightly slower than uninjected embryos, and staging was performed based on anatomical landmarks. The 5E1 antibody-injected embryos largely exhibit a normal gross morphology, although at least half of them have a smaller head compared to control (Fig. 3B). Similar cephalic phenotypes have been reported (Ahlgren and Bronner-Fraser, 1999). Embryos injected with control 12CA5 hybridoma cells have a macroscopic and microscopic anatomy identical to untreated embryos.

Vessel Malformations in Anti-Shh Antibody-Treated Embryos

Even at the anatomical level, the effect of inhibiting Shh on vessel development is remarkable. Generally, in embryos injected with 5E1 hybridoma cells development of the aortic arches is delayed. While in stage-18 control embryos, the first and the second aortic arches start to regress into capillary plexi, these aortic arches are still present in 5E1-injected embryos, indicating a delay in remodeling (Fig. 3A,B).

A consequence of Shh inhibition is the failure of the anterior cardinal vein and its branches to form functional vessel walls. Hemorrhages were observed frequently (Fig. 3A–D), and these vessels were permeable to ink, unlike the control hybridoma-injected

animals, which were able to contain the ink within the vessels (Fig. 3A,B). In addition to the ink-permeability, the lumen of either anterior cardinal vein in 5E1-injected embryos is sinusoidal with endothelium-lined protrusions (Fig. 4A–D). This demonstrates that Shh plays an important role in the establishment of a functional wall in the anterior cardinal veins and its tributaries.

Several arteries show abnormal development as a consequence of 5E1 injection as well. The internal carotid arteries are characterized by the presence of a transverse septum over a length of up to 40 μm (in 2 of 6 embryos). This septum consists of two layers of endothelium, with mesenchyme in between, dividing the internal carotid artery into two separate vessels, which merge again further rostrally (Fig. 4E–G). Similarly, an abnormal septum is present in the dorsal aorta (in 4 out of 6 embryos). This aortic septum is usually about 60 μm long, and is covered with endothelium on both sides (Fig. 4H–J). Although we assume that this septation is a result of delayed fusion, it remains possible that it has formed after the initial fusion of the left and right dorsal aortae. The same domain of the dorsal aorta in control embryos is already fused and has a single lumen. Vessel abnormalities are also found in outflow tracts of the heart. Besides vessels with irregular lumina and unusual invaginations (Fig. 4N–P), we have also observed curving strands of endothelial cells in successive sections, possibly malformed vessels with an incomplete vessel wall (Fig. 4K–M) (in 4 of 6 embryos). Embryos injected with the control hybridoma cells had no obvious vessel malformations.

To further assess malformations in vessel endothelium, we determined the expression VEGFR2, which is expressed in endothelial cells (Jaffredo et al., 1998) albeit not ubiquitously. At stage 18, VEGFR2 is expressed in all endothelial cells of small developing vessels as capillaries, such as brain capillaries, while only about half the endothelial cells of bigger arteries express VEGFR2. Similarly, the dorsal aorta is lined by VEGFR-positive cells, but only in its ventrolateral aspect, where the aortic arches are con-

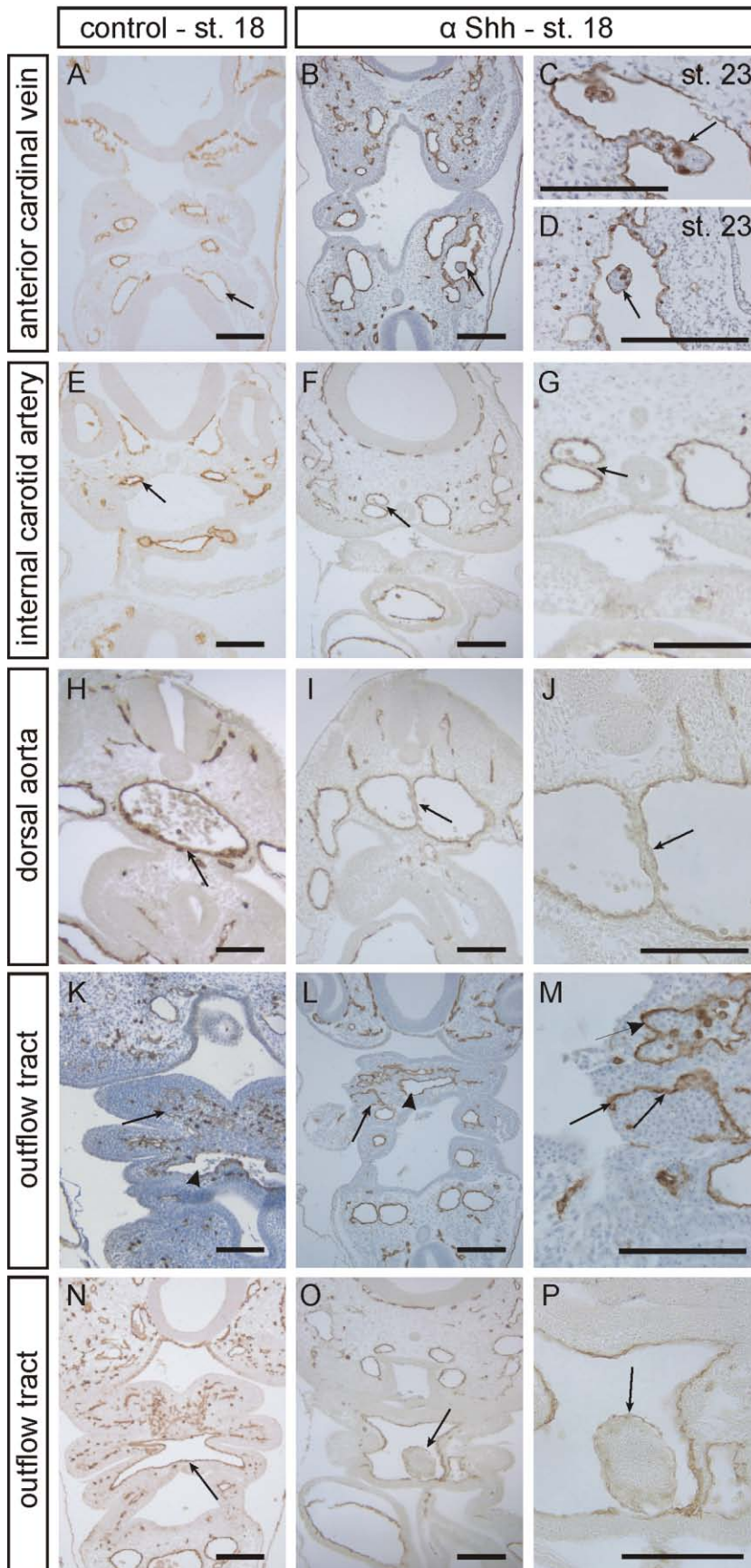


Fig. 4.

ected. Besides endothelial cells, VEGFR2 is highly expressed in the outflow tract myocardium, while outflow tract endothelium contains only few VEGFR2-positive cells. These myocardial cells are probably derived from endothelium (Wilting et al., 1997). VEGFR2 was also expressed in the notochord, as it was previously reported (Nimmagadda et al., 2004). We did not detect any difference in VEGFR2 expression in 5E1-injected embryos compared to control, indicating that VEGF is not a critical mediator of the effects of Shh (not shown).

Following the formation of an endothelial layer, the smooth muscle cells start to surround the forming vessels. At stage 18, smooth muscle cells completely cover the endothelial lining of the dorsal aorta and the internal carotid arteries (Fig. 4A). The aortic arches have smooth muscle cells only on their lateral side, while an incomplete layer of smooth muscle cells is associated with the outflow tract. Smooth muscle actin is also present in the myotome (Fig.

Fig. 4. QH1 staining of vessel endothelium showing lumen malformations in anti-Shh hybridoma cell-injected embryos. **A–D:** Lumen malformation in the anterior cardinal vein. **A:** Control embryo. **B:** The anterior cardinal vein exhibits irregularities and contains protrusions of the endothelial layer extending into the vessel lumen (arrow) at stage 18. **C, D:** Protrusions in the anterior cardinal vein (arrow) are also found in embryos injected with anti-Shh antibody and harvested at stage 23. **E–G:** Internal carotid artery malformations at stage 18. **E:** Control embryo. **F:** The internal carotid artery is divided by a horizontal septum (arrow) into two separate vessels. **G:** Detail of septum covered in endothelium from both sides (arrow). **H–J:** Dorsal aorta malformations, stage 18. **H:** Control embryo. **I:** Failure of complete fusion between the left and right dorsal aortae. The persistent septum is indicated (arrow). **J:** Detail of septum (arrow). **K–M:** Malformations of outflow tract endothelium at stage 18. **K:** Control embryo. **L:** The endothelium of the outflow tract fails to form a lumenized vessel (arrow), and instead forms an isolated endothelial wall with red blood cells on one side. **M:** Detail of patent vessel endothelium (arrow) and adjacent malformed vessel (arrow). **N–P:** Malformations of the outflow tract at stage 18. **N:** Control embryo. **O:** The outflow tract has developed a protrusion of tissue surrounded by the endothelial layer, which invaginates into the lumen (arrow). **P:** Detailed view of the endothelial protrusion (arrow). Transversal sections. **B–D, K–M** are counterstained with hematoxylin. Scale bar = 400 μ m in all panels.

5C). At stage 23, a continuous smooth muscle layer surrounds aortic arches and the outflow tracts (Fig. 5E). Also, all branches of the internal carotid arteries have a continuous layer of smooth muscle cells, while the anterior cardinal veins and their tributaries are devoid of smooth muscle cells. The formation of the smooth muscle cell lining of the vessels is unaffected by injection of 5E1 hybridoma cells (Fig. 5B,F), despite the presence of obvious vessel malformations. Smooth muscle cells also line the abnormal aortic septum (Fig. 5D). This is consistent with our observation that the formation of the smooth muscle lining of the vessels is unaffected by injection of 5E1 hybridoma cells (Fig. 5B,F), despite the presence of obvious vessel malformations. Smooth muscle cells also line the abnormal aortic septum (Fig. 5D). This is consistent with our observation that the formation of the smooth muscle lining of the dorsal aortae precedes the subsequent fusion of these vessels. Altogether, this indicates that the loss of Shh signaling has little effect on the process in which smooth muscle cells form around new vasculature.

Angiogenic and Macrophage-Like Cells in Anti-Shh Antibody-Treated Embryos

The main effect of conditional Shh inhibition on blood vessel development in embryos injected at later stages (injected in stage 13–15 and harvested at stage 21–23) is the presence of an increased number of free, round endothelial cells, positive for QH1. These cells are not integrated into functional vessel lumina, but aggregate into multicellular clusters. Such aggregates usually are found around the anterior cardinal veins, around the dorsal aorta, and in the branchial arches around the aortic arches. Such cell aggregates are not present in control 12CA5 hybridoma-injected embryos, where angiogenic cells are fewer and isolated. The increased number of aggregates is most significant in the sixth branchial arch (Fig. 6G–L), around the anterior cardinal vein, and just ventral to the dorsal aorta (Fig. 7A–L), while the anterior branchial arches are the least affected. In the first and second branchial arch, we have not observed any significant difference compared to control in the number of endothelial cell aggregates (data not shown). This might either indicate that at the moment of injection the Shh re-

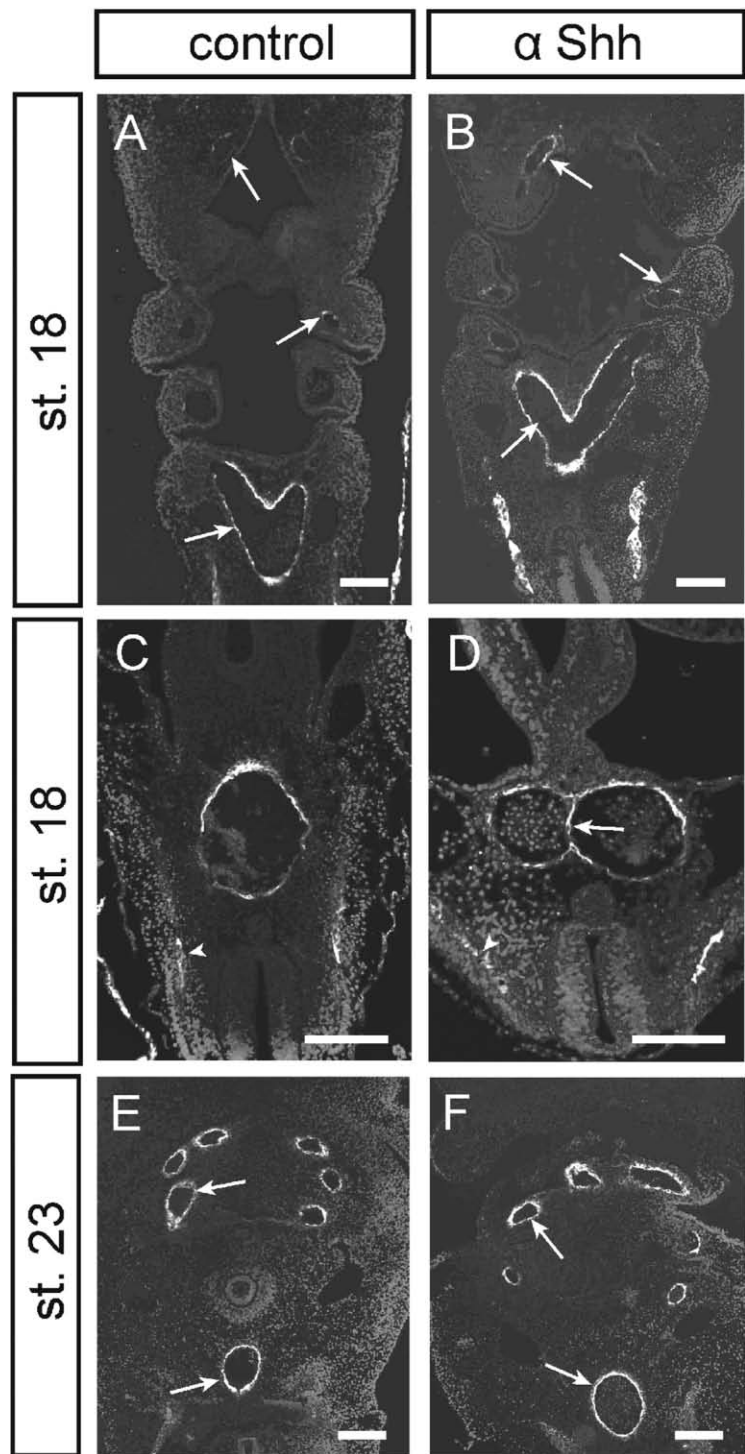


Fig. 5. Distribution of vascular smooth muscle cells visualized with smooth muscle actin Ab. **A,B:** Smooth muscle cells in a stage-18 embryo are present around the dorsal aorta, internal carotid artery, and the lateral part of the aortic arches (arrows). 5E1-injected embryos show no difference in the distribution of smooth muscle cells (B) compared to control injected embryos (A). Scale bar = 400 μm . **C,D:** Stage-18 embryos. Smooth muscle cells also cover the endothelial malformation caused by 5E1 injection. **C:** Normal dorsal aorta. **D:** Persistent septum in the dorsal aorta (arrow). Arrowheads show expression of the smooth muscle actin in the myotome. Scale bar = 400 μm . **E,F:** Smooth muscle cells in a stage-23 embryo are present in the dorsal aorta, internal carotid artery, aortic arches, and the outflow tracts (arrows). 5E1-injected embryos show no difference in the distribution of the smooth muscle cells (F) compared to control-injected embryos (E). Scale bar = 200 μm .

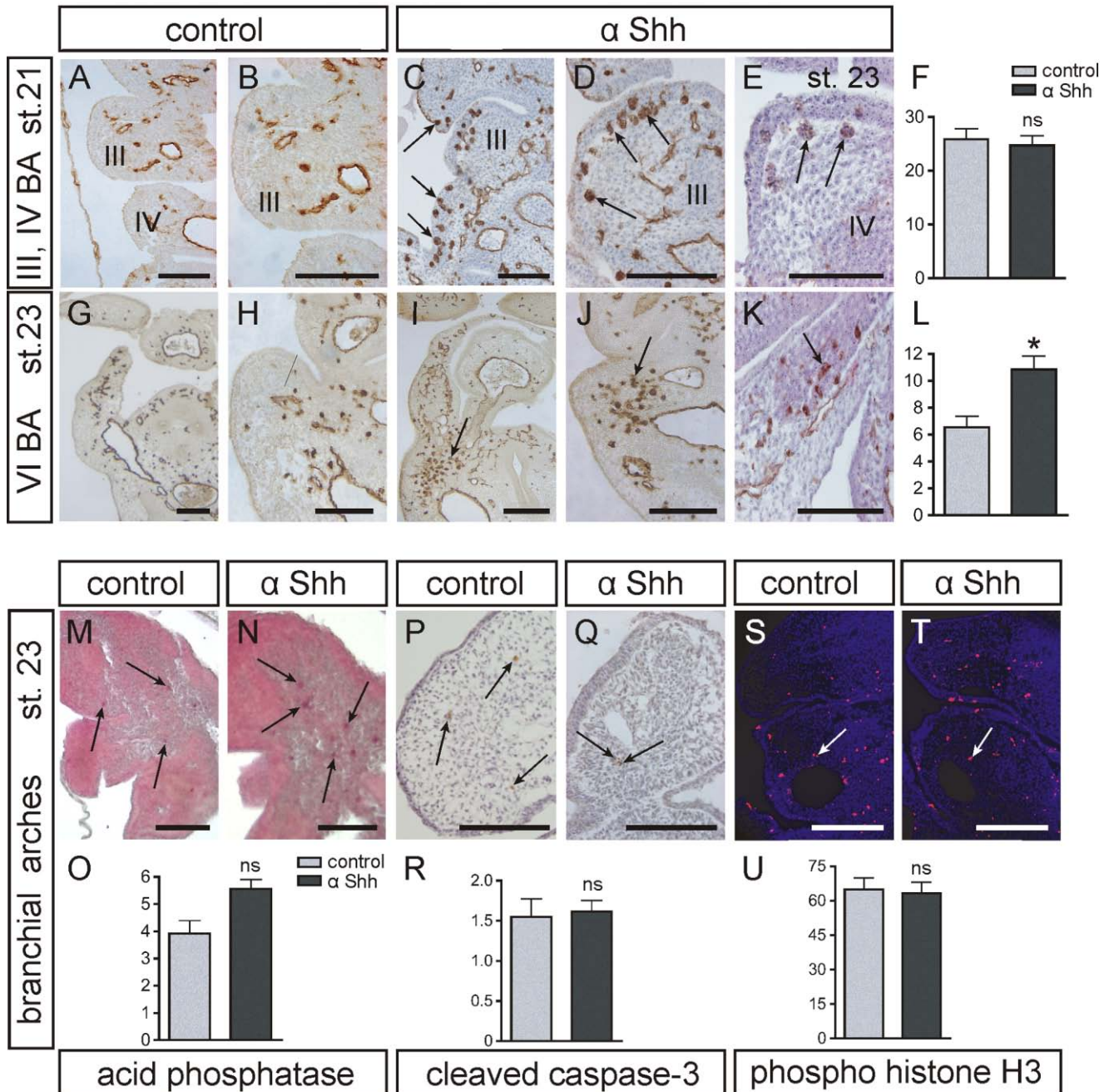


Fig. 6. QH1-positive cell abnormalities in branchial arches at stage 21 (A–D, F) and stage 23 (E, G–U); Characterization of QH1-positive cells: macrophage-like cells stained for acid phosphatase (M–O); apoptotic cells positive for cleaved caspase-3 (P–R); proliferating cells positive for phospho histone H3 (S–U). A–F: QH1-positive cells in the mesenchyme and ectoderm of third and fourth branchial arches at stage 21 (stage 23–E). **A,B:** Control embryos. **C,D:** Larger aggregates of QH1-positive cells (arrows) in anti-Shh-injected embryos at stage 21 or (E) stage 23. **F:** Graph shows that anti-Shh-treated embryos have a similar number of QH1-positive cells as the controls. However, QH1-positive cells are present in large aggregates compared to single cells in control embryos. Y-axis: average number of QH1-positive cell aggregates in the third and fourth branchial arches. G–L: Increased number of QH1-positive cells in the sixth branchial arch of stage-23 embryos injected with anti-Shh hybridoma cells. **G,H:** Control embryos. **I:** QH1-positive cells (arrows) in the distal region of the sixth branchial arch and (J) detail. **K:** Increased number of QH1-positive cells (arrows) in the proximal region of the branchial arch. **L:** Graph shows the increased number of QH1-positive cells in anti-Shh-injected embryos in the sixth branchial arch. Y-axis: average number of QH1-positive cell aggregates in the sixth branchial arch. **M–O:** Very few macrophage-like cells are present in the branchial arches. Anti-Shh injection has no significant effect on the number of macrophage-like cells (O). **P–R:** No significant difference in the number of apoptotic cells (arrow) in response to anti-Shh injection (R). **S–U:** No significant difference in the number of proliferating cells in the branchial arches in anti-Shh injected embryos (arrows). Transversal sections. C–E, K, P, Q counterstained with hematoxylin. Scale bar = 200 μ m in all panels. Graphs: Standard deviation is indicated. *Significant difference ($P < 0.05$); ns, no significant difference.

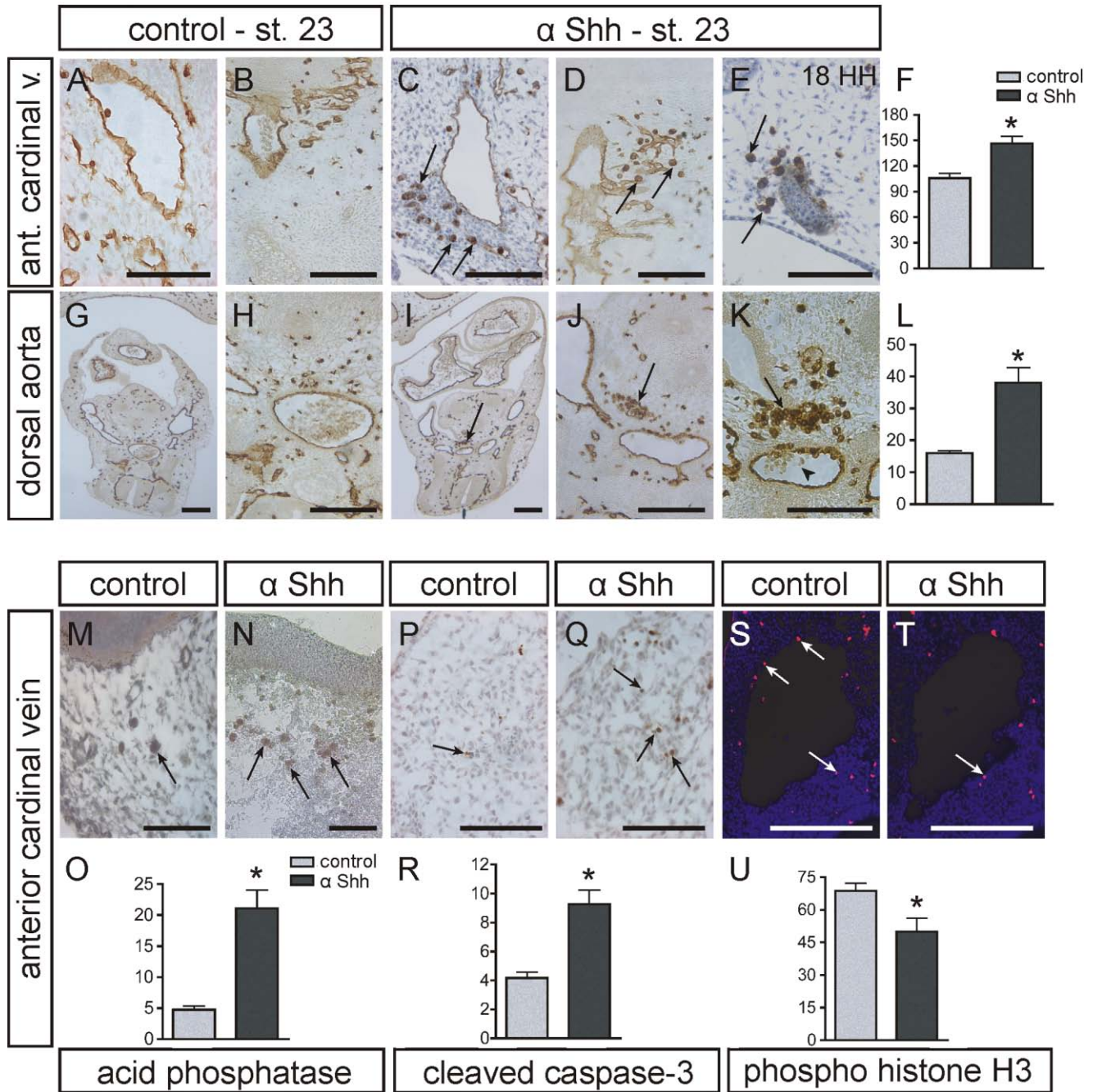


Fig. 7. Abnormalities in the number of QH1-positive cells around the main vessel trunks at stage 23: the anterior cardinal vein and the dorsal aorta (A–L); Characterization of QH1-positive cells: macrophage-like cells stained for acid phosphatase (M–O); apoptotic cells positive for cleaved caspase-3 (P–R); proliferating cells positive for phospho histone H3 (S–U). A–F: Anterior cardinal vein malformations. **A, B:** Control embryos. **C:** Increased number of QH1-positive cells around the anterior cardinal vein (arrows) in anti-Shh hybridoma cell-injected embryos. **D:** Increased number of QH1-positive cells around a branch of the anterior cardinal vein (arrows). **E:** Free QH1-positive cells are present around the anterior cardinal vein already at stage 18 (arrows). **F:** Graph showing a higher number of QH1-positive cells in the anterior cardinal vein region in embryos injected with anti-Shh antibody. Y-axis: average number of QH1-positive cells per section. Standard deviation is indicated. **G–L:** Increased number of QH1-positive cells around the dorsal aorta at stage 23. **G, H:** Control embryos. **I:** Aggregate of QH1-positive cells on the ventral side of the dorsal aorta (arrow) and (**J**) detail of the aggregate (arrow). **K:** QH1-positive cells are present (arrow), but hematopoietic regions in dorsal aorta appear normal (arrowhead). **L:** Graph shows the increased number of QH1-positive cells in anti-Shh-injected embryos in the dorsal aorta region. Y-axis: average number of QH1-positive cells per field. Standard deviation is indicated. **M–O:** Increased number of macrophage-like cells stained with acid phosphatase (arrows) in the region of the anterior cardinal vein in anti-Shh-injected embryos. **O:** Graph indicating the increased number of macrophage-like cells. **P–R:** Increased number of cleaved Caspase-3 (apoptotic) cells (arrows) around the anterior cardinal vein in anti-Shh-injected embryos. **R:** Graph showing the increased number of apoptotic cells. **S–U:** Decreased number of dividing cells (arrows) in the anterior cardinal vein region in anti-Shh-injected embryos. **U:** Graph showing the difference in proliferating cells. Transverse sections. C, E, P, Q, counterstained with hematoxylin; M, N, counterstained with Fast green. Scale bar = 200 μ m in all panels. Graphs: Y-axis: average number of positive cells per field. Standard deviation is indicated; *significant difference ($P < 0.05$).

quirement for initial vessel formation has passed, or that the absence of de-novo vascularization associated with the regression of the first and second aortic arches results in an absence of these aggregates of QH1-positive cells.

In the third and fourth branchial arches, Shh inhibition results in an increased number of larger endothelial aggregates compared to 12CA5-injected control embryos. These aggregates are mainly localized in the mesenchyme, sometimes in close proximity to branchial arch ectoderm and endoderm. Such aggregates are not present in control embryos, where we observed only solitary QH1-positive cells, in comparable numbers to the solitary cells in anti-Shh-treated embryos (Fig. 6A–F).

The sixth branchial arch is the most affected as measured by the number of QH1-positive cells not part of an obvious vessel wall. These cells are present along the whole extent of the arches and are concentrated in mesenchyme as aggregates and solitary cells. In control embryos, only solitary QH1-positive cells are observed. The total number of nonintegrated QH1-positive cells is significantly higher in 5E1 hybridoma-injected embryos than in controls (Fig. 6G–L).

The biggest increase of nonintegrated endothelial cells as a consequence of 5E1 injection is detected ventral to the dorsal aorta (Fig. 7G–L). It is possible that this abundance of angiogenic cells is related to the area of hemangiogenesis within the wall of the ventral aorta (Jaffredo et al., 1998). Increased numbers of endothelial cell aggregates were also found in the vicinity of the anterior cardinal veins. The QH1-positive cells in this area (Fig. 7A–F) are the only cells that are predominantly identified as macrophage-like cells, rather than angiogenic cells (Fig. 6M–O). Macrophage-like cells are the phagocytic cells of the early embryo, are derived from hemangioblasts (Cuadros et al., 1992), and are characterized by their expression of acid phosphatase (Fig. 7M–O). Direct co-localization of acid phosphatase and QH1 staining is not possible due to incompatible fixation and processing requirements.

Apoptosis and Proliferation in Anti-Shh Ab-Treated Embryos

In many instances during development, loss of Shh leads to decreased proliferation and increased apoptosis, possibly explaining some of the vessel malformations we observed as a consequence of 5E1 injection.

A significant increase in the number of apoptotic, caspase-3-positive cells (Fig. 7P–R) is observed around the anterior cardinal veins in 5E1-injected embryos, suggesting a role for Shh in cell survival in this region and, consequently, an increased number of macrophage-like cells is detected. In contrast, in the branchial arches and around the dorsal aorta, the frequency of cleaved caspase-3-positive apoptotic cells do not differ from control embryos (Fig. 6P–R). Since the domains of apoptosis coincide with the areas where vessel integrity is compromised, it remains a possibility that the hemorrhages increase apoptosis in the surrounding tissues (Figs. 6, 7S–U).

Coincident with the increased apoptosis, we observed decreased proliferation near the anterior cardinal vein (Figs. 5, 6S–U), but not in the other regions studied.

DISCUSSION

The widespread expression of Shh in endoderm, floor plate, and notochord, as well as the proximity of the dorsal aortae, anterior cardinal veins, and aortic arches to these Shh-producing structures, prompted us to assess the role of Shh signaling in pharyngeal vessel development.

Previous examinations of *Shh* null embryos (Jeong et al., 2004; Yamagishi et al., 2006) have demonstrated a Shh requirement for normal branchial arch formation. However, global defects in these animals prevent assessment of the involvement of Shh in later stages of branchial arch development (Washington Smoak et al., 2005). Using a method of inhibiting Shh response at later developmental stages, we demonstrate a continual requirement for Shh for the correct formation of the pharyngeal vasculature. Taking advantage of the anterior-posterior developmental gradient of the branchial arches, we could si-

multaneously study the effects of Shh inhibition in the further developed anterior branchial arches (I–III) as well as the newly formed posterior arches (IV–VI). In the posterior arches, we observed a failure of vessel luminization, represented by formation of numerous aggregates of endothelial cells. This shows Shh requirement in the early stages of vessel development. A similar effect that blocked Shh signaling in the early stages of vasculogenesis was observed before mice and chick embryos (Vokes and Krieg, 2002; Vokes et al., 2004).

Already formed vessels are affected by Shh inhibition in their remodeling. This effect is characterized by delayed fusion, impaired branching, and unusual invaginations of the vessel walls. Such malformations are observed in the dorsal and ventral aorta, the internal carotid arteries, and anterior cardinal veins, which are actively remodeled at that time. These disturbances of vessel remodeling are not known to be affected by Shh signaling, although it has been observed that cyclopamine treatment affected fusion of the dorsal aortae (Nagase et al., 2006). Alterations of vessel remodeling are found in arteries that have already formed smooth muscle layer. However, the wall of malformed anterior cardinal veins does not contain smooth muscle cells. This suggests that the presence or absence of a smooth muscle layer does not play a critical role in the generation of vessel malformations. These results show that Shh is essential to maintain the stability and coherence of the endothelial layer of the veins, as we detected in the anterior cardinal vein. A similar phenotype is observed in zebrafish with disrupted Shh signaling (S.J. Childs personal communication).

In our study, we expected to find increased level of apoptosis and decreased proliferation as a consequence of Shh signal attenuation, as it was reported by previous observation at earlier stages of avian development (Ahlgren and Bronner-Fraser, 1999) and in mice (Jeong et al., 2004; Washington Smoak et al., 2005). However, our results do not generally show this effect. We observed increased level of apoptosis and decreased proliferation only around the anterior cardinal veins at stage 23. At stage 18, there

was no significant difference in numbers of proliferating and apoptotic cell between control and Shh-inhibited embryos (data not shown). It seems, thus, that Shh signaling influences cell proliferation and survival more profoundly at earlier developmental stages.

Interestingly, sources of Shh are not necessarily in the direct vicinity of the vessels affected by the application of 5E1 anti-Shh hybridoma cells. There are several sites of Shh expression in the vicinity of the anterior cardinal veins, including the floorplate of the hindbrain and midbrain, the domains of Shh expression in the forebrain, as well as the notochord and the prechordal plate. Shh derived from the notochord and floor plate influences dorsal aortic development (Nagase et al., 2006), and it remains unsolved how Shh reaches these distant sites. Intermediary factors such as Angiopoietin-1, VEGFs (Pola et al., 2001), Fox1, and BMP4 (Jeong et al., 2004; Astorga and Carlsson, 2007) could mediate the effects of Shh. However, direct signaling of Shh to the endothelial is likely to occur, consistent with the relatively large area over which *Ptch1* expression is decreased after Shh inhibition. Also, the Shh independence of VEGFR2 expression indicates that VEGF does not play a critical intermediary role between Shh and its effect on the endothelial cells, altogether supporting a model in which Shh signals the vessel endothelium directly. Furthermore, in experiments with mutant mice, in which neural crest-derived mesenchyme in the branchial arches was rendered insensitive to Hh signaling, initial vascularization appeared normal (Sasai et al., 2001; Jeong et al., 2004), showing that a possible intermediary signal is not generated in crest-derived mesenchyme. However, the possible role of non-crest mesenchymal cells remains to be determined.

In conclusion, our results demonstrate a continual requirement for Shh signaling for vascular development and remodeling. We have observed minor differences at best in apoptosis and proliferation, and no difference in smooth muscle actin and VEGFR2 expression, supporting the idea that Shh acts directly on vessel endothelium and not via intermedi-

aries induced in the mesenchyme between the Shh sources and the vessels. Nevertheless, the molecular events following the initial Shh response, which instructs endothelial cells to form blood vessels, remains to be solved.

EXPERIMENTAL PROCEDURES

Embryos

Fertilized quail (*Coturnix coturnix japonica*) eggs were obtained from the Research Institute of Animal Production, Prague, Czech Republic, and from B&D Farm (Harrah, OK). For in situ hybridization of *Ptch1* mRNA, we used chick embryos. Eggs were incubated at 38°C and embryos ranging from stage 6 to 23, as defined by Hamburger and Hamilton (1951) (23–100 hr of incubation), were studied. We injected over 150 embryos with 5E1 hybridoma cells. As a control, we used approximately 100 embryos injected with 12cA5 hybridoma cells and as an additional control we used uninjected embryos.

Immunohistochemistry and Histochemistry

Shh was detected in cryostat sections derived from embryos fixed in 4% Phosphate Buffered Paraformaldehyde using monoclonal antibody 5E1 (Hybridoma Bank) diluted at 1:50. As a secondary antibody, Goat anti-Mouse Biotin (Sigma B7264) (1:500) was used and tertiary antibody was Extravidin Px (Sigma 2886) (1:100) and DAB (Sigma D5905) as a chromogen.

The endothelium of vessels was visualized with monoclonal antibody QH1 (Hybridoma Bank) in paraffin sections (1:1,000). As a secondary antibody, we used Goat anti-Mouse Px IgG (Sigma A 4416) and the reaction product was detected with DAB. Alternatively, endothelium was visualized with VEGFR2 monoclonal antibody (kindly provided by Dr. Eichmann; Eichmann et al., 1997) diluted 1:1 in the cryostat sections. For enhancing the signal Tyramide Signal Amplification system (TSA, Dako) was used according to the manufacturer's recommendation except that Strepta-

vidin peroxidase was used rather than Extravidin peroxidase as it decreased background levels significantly. As a secondary antibody, Rabbit anti mouse IgG1-Biotin was used.

Apoptosis was detected with Anti-Cleaved Caspase-3 monoclonal antibody (BD Pharmingen 559565) at 1:500, in paraffin sections and cryosections. The secondary antibody was Goat anti-Rabbit Biotin (1:500) and tertiary antibody was Extravidin Px (Sigma 2886) (1:100), and visualized using DAB.

Proliferating cells were detected with anti-Phospho Histone H3 polyclonal antibody (Upstate 06570) 1:200 in cryosections. As a secondary antibody we used Goat-anti Rabbit Rhodamine (Cappel Pharmaceutical) (1:500).

Periendotelial smooth muscle cells were detected using anti-smooth muscle actin Ab (Sigma A2547) 1:500 and Goat anti Mouse TRITC as a secondary Ab (1:150). Phagocytic function of macrophage-like cells was detected with histochemical staining for Acid Phosphatase resistant to Tartaric Acid. Embryos were fixed in acetone overnight at 4°C, transferred into xylene, and subsequently embedded in paraffin. Sections were deparaffinized with xylene and rehydrated through acetone and acetone/distilled water (1:1). Sections were incubated overnight at room temperature in solution prepared with 10 mg of Naphtol-AS-BI phosphate (Sigma, 70491-Fluka) in 0.5 ml N,N-dimethyl formamide. This solution was resuspended in 50 ml of 0.1M acetic acid buffer, pH 5.2 (Walpole acetate), and 20 mg of Fast Red Violet (Sigma, F3381) was added, as well as a minimum of 140 mg of Tartaric Acid (Sigma Aldrich, 14314DE).

mRNA In Situ Hybridization

A plasmid containing chick *Ptch1* (clone 200; a gift from M. Scott) (Xie et al., 1997) was linearized with SalI and transcribed using T3 polymerase. Hybridization in situ on paraffin sections was carried out as described (Nieto et al., 1996; Nanka et al., 2006).

Vascular System Ink Injection

The vascular system was visualized in vivo by injecting black ink diluted 1:20

in PBS via the vitelline vein using a glass capillary. The beating heart distributed the ink completely throughout the vascular system. After injection, embryos were collected, fixed in 4% PFA, and analyzed.

Inhibition of Shh Function With Anti-Shh (5E1) Antibody

Just before the injection, around 10^8 hybridoma cells were collected by centrifugation and resuspended in about 200 μ l of Liebovitz L-15 medium (Sigma). This suspension was loaded into a small capillary and injected under the vitelline membrane near the branchial region of quail and chick embryos. Injecting the cells to the paraxial mesoderm caused the same level of Shh inhibition as with injection in the proximity of branchial arches, which is less invasive. After injection, embryos were incubated for 1 to 3 days and isolated for analysis. Embryos were either injected at stages 10–12 and re-incubated either until they reached stage 18 or 21–23, or embryos were injected at stage 13–15 embryos and incubated until stage 21–23. We used either 5E1 anti-Shh mouse hybridoma or 12CA5 mouse hybridoma cells, which produce an anti-HA antibody (Handley-Gearhart et al., 1994).

Quantification

QH1-positive cell aggregates and cells not integrated into the endothelial layer, macrophage-like cells positive for acid phosphatase, apoptotic cells exhibiting cleaved caspase-3 Ab, and proliferating cells positive for Phospho Histone-3, were counted. Counting was performed on serial 10- μ m sections from the following morphological regions: each branchial arch, dorsal aorta, anterior cardinal vein, and outflow tract regions. The dorsal aorta region includes its surrounding structures ventrally to the sixth branchial arch, the liver primordium, and dorsally up to the neural tube. The anterior cardinal vein region includes all anterior structures besides the eye and brain, and the area ventral to the first branchial arch and the oral cavity. The outflow tract region includes area of vessels and mesenchyme,

starting caudally in the heart and continuing cranially to the branchial arches.

Cells were counted in every fourth section, at a minimum of 20 sections per region. Six embryos were analyzed for the number of QH1-positive cells, four embryos for macrophage-like cells and for apoptotic cells and two embryos for the number of proliferating cells. Counts were averaged and the standard deviation was determined.

ACKNOWLEDGMENTS

We thank Ms. E. Kluzáková, M. Pleschnerová, A. Kvasilová, and Mr. M. Tsma for excellent technical assistance. This work was supported by GAUK 54/203209 (Grant Agency of Charles University) to Hana Kolesová, by MSM 0021620806 (project from The Ministry of Education of The Czech Republic) to Miloš Grim, and by NIH grant 1R01HD042307 to Henk Roelink.

REFERENCES

- Ahlgren SC, Bronner-Fraser M. 1999. Inhibition of sonic hedgehog signaling in vivo results in craniofacial neural crest cell death. *Curr Biol* 9:1304–1314.
- Astorga J, Carlsson P. 2007. Hedgehog induction of murine vasculogenesis is mediated by Foxf1 and Bmp4. *Development* 134:3753–3761.
- Byrd N, Becker S, Maye P, Narasimhaiah R, St-Jacques B, Zhang X, McMahon J, McMahon A, Gabel L. 2002. Hedgehog is required for murine yolk sac angiogenesis. *Development* 129:361–372.
- Carpenter D, Stone DM, Brush J, Ryan A, Armanini M, Frantz G, Rosenthal A, de Sauvage FJ. 1998. Characterization of two patched receptors for the vertebrate hedgehog protein family. *Proc Natl Acad Sci USA* 95:13630–13634.
- Cuadros MA, Coltey P, Carmen Nieto M, Martin C. 1992. Demonstration of a phagocytic cell system belonging to the hemopoietic lineage and originating from the yolk sac in the early avian embryo. *Development* 115:157–168.
- Eichmann A, Corbel C, Nataf V, Vaigot P, Breant C, Le Douarin NM. 1997. Ligand-dependent development of the endothelial and hemopoietic lineages from embryonic mesodermal cells expressing vascular endothelial growth factor receptor 2. *Proc Natl Acad Sci USA* 94:5141–5146.
- Evans DJ, Noden DM. 2006. Spatial relations between avian craniofacial neural crest and paraxial mesoderm cells. *Dev Dyn* 235:1310–1325.

- Goodrich LV, Milenkovic L, Higgins KM, Scott MP. 1997. Altered neural cell fates and medulloblastoma in mouse patched mutants. *Science* 277:1109–1113.
- Hamburger V, Hamilton HL. 1951. A series of normal stages in the development of the chick embryo. *J Morphol* 88:49–90.
- Handley-Gearhart PM, Stephen AG, Trausch-Azar JS, Ciechanover A, Schwartz AL. 1994. Human ubiquitin-activating enzyme, E1. Indication of potential nuclear and cytoplasmic subpopulations using epitope-tagged cDNA constructs. *J Biol Chem* 269:33171–33178.
- Hiruma T, Hirakow R. 1995. Formation of the pharyngeal arch arteries in the chick embryo. Observations of corrosion casts by scanning electron microscopy. *Anat Embryol (Berl)* 191:415–423.
- Jaffredo T, Gautier R, Eichmann A, Dieterlen-Lievre F. 1998. Intraaortic hemopoietic cells are derived from endothelial cells during ontogeny. *Development* 125:4575–4583.
- Jeong J, Mao J, Tenzen T, Kottmann AH, McMahon AP. 2004. Hedgehog signaling in the neural crest cells regulates the patterning and growth of facial primordia. *Genes Dev* 18:937–951.
- Kolesova H, Lametschwandtner A, Rocek Z. 2007. The evolution of amphibian metamorphosis: insights based on the transformation of the aortic arches of *Pelobates fuscus* (Anura). *J Anat* 210:379–393.
- Le Lievre CS, Le Douarin NM. 1975. Mesenchymal derivatives of the neural crest: analysis of chimaeric quail and chick embryos. *J Embryol Exp Morphol* 34:125–154.
- Marigo V, Tabin CJ. 1996. Regulation of patched by sonic hedgehog in the developing neural tube. *Proc Natl Acad Sci USA* 93:9346–9351.
- Nagase T, Nagase M, Yoshimura K, Machida M, Yamagishi M. 2006. Defects in aortic fusion and craniofacial vasculature in the holoprosencephalic mouse embryo under inhibition of sonic hedgehog signaling. *J Craniofac Surg* 17:736–744.
- Nanka O, Valasek P, Dvorakova M, Grim M. 2006. Experimental hypoxia and embryonic angiogenesis. *Dev Dyn* 235:723–733.
- Nieto MA, Patel K, Wilkinson DG. 1996. In situ hybridization analysis of chick embryos in whole mount and tissue sections. *Methods Cell Biol* 51:219–235.
- Nimmagadda S, Loganathan PG, Wilting J, Christ B, Huang R. 2004. Expression pattern of VEGFR-2 (Quek1) during quail development. *Anat Embryol (Berl)* 208:219–224.
- Noden DM, Trainor PA. 2005. Relations and interactions between cranial mesoderm and neural crest populations. *J Anat* 207:575–601.
- Pardanaud L, Yassine F, Dieterlen-Lievre F. 1989. Relationship between vasculogenesis, angiogenesis and haemopoiesis during avian ontogeny. *Development* 105:473–485.

- Pola R, Ling LE, Silver M, Corbley MJ, Kearney M, Pepinsky RB, Shapiro R, Taylor FR, Baker DP, Asahara T, Isner JM. 2001. The morphogen Sonic hedgehog is an indirect angiogenic agent up-regulating two families of angiogenic growth factors. *Nature Medicine* 7:706–711.
- Roelink H, Porter JA, Chiang C, Tanabe Y, Chang DT, Beachy PA, Jessell TM. 1995. Floor plate and motor neuron induction by different concentrations of the amino-terminal cleavage product of sonic hedgehog autoproteolysis. *Cell* 81:445–455.
- Sasai N, Mizuseki K, Sasai Y. 2001. Requirement of FoxD3-class signaling for neural crest determination in *Xenopus*. *Development* 128:2525–2536.
- van Tuyl M, Groenman F, Wang J, Kuliszewski M, Liu J, Tibboel D, Post M. 2007. Angiogenic factors stimulate tubular branching morphogenesis of sonic hedgehog-deficient lungs. *Dev Biol* 303:514–526.
- Vokes SA, Krieg PA. 2002. Endoderm is required for vascular endothelial tube formation, but not for angioblast specification. *Development* 129:775–785.
- Vokes SA, Yatskievych TA, Heimark RL, McMahon J, McMahon AP, Antin PB, Krieg PA. 2004. Hedgehog signaling is essential for endothelial tube formation during vasculogenesis. *Development* 131:4371–4380.
- Washington Smoak I, Byrd NA, Abu-Issa R, Goddeeris MM, Anderson R, Morris J, Yamamura K, Klingensmith J, Meyers EN. 2005. Sonic hedgehog is required for cardiac outflow tract and neural crest cell development. *Dev Biol* 283:357–372.
- Wiegrefe C, Christ B, Huang R, Scaal M. 2007. Sclerotomal origin of smooth muscle cells in the wall of the avian dorsal aorta. *Dev Dyn* 236:3191–3192.
- Wijgerde M, McMahon JA, Rule M, McMahon AP. 2002. A direct requirement for Hedgehog signaling for normal specification of all ventral progenitor domains in the presumptive mammalian spinal cord. *Genes Dev* 16:2849–2864.
- Wilting J, Eichmann A, Christ B. 1997. Expression of the avian VEGF receptor homologues Quek1 and Quek2 in blood-vascular and lymphatic endothelial and non-endothelial cells during quail embryonic development. *Cell Tissue Res* 288:207–223.
- Xie J, Johnson RL, Zhang X, Bare JW, Waldman FM, Cogen PH, Menon AG, Warren RS, Chen LC, Scott MP, Epstein EH, Jr. 1997. Mutations of the PATCHED gene in several types of sporadic extracutaneous tumors. *Cancer Res* 57:2369–2372.
- Yamagishi C, Yamagishi H, Maeda J, Tsuchihashi T, Ivey K, Hu T, Srivastava D. 2006. Sonic hedgehog is essential for first pharyngeal arch development. *Pediatr Res* 59:349–354.
- Zhang XM, Ramalho-Santos M, McMahon AP. 2001. Smoothed mutants reveal redundant roles for Shh and Ihh signaling including regulation of L/R asymmetry by the mouse node. *Cell* 105:781–792.